Conformation and thermal inversion of 10,11-dihydro-5*H*-dibenzo[*a*,*d*]cycloheptene ring spiro-linked to homoquinones †

Takumi Oshima,*[a] Schunpei Fujii,[a] Toshihiko Takatani,[a] Ken Kokubo[a] and Tatsuya Kawamoto[b]

[a] *Department of Applied Chemistry, Faculty of Engineering, Osaka University, Toyonaka 560, Japan*
[b] *Department of Chemistry, Graduate School of Science, Osaka University, Toyonaka 560, Japan*

Received (in Cambridge) 18th January 1999, Accepted 21st May 1999

1,3-Dipolar cycloaddition of 5-diazo-10,11-dihydro-*5H*-dibenzo[*a*,*d*]cycloheptene with 2,5-dimethyl-1,4-benzoquinone gave the less stable conformer of 10′,11′-dihydro-1,4-dimethylspiro[bicyclo[4.2.0]hept-3-ene-7,5′-(5′*H*-dibenzo[*a*,*d*]cycloheptene)]-2,5-dione (α-conformer) *via* a conformationally retained nitrogen extrusion from the sterically congested indazole adduct. X-Ray structure analyses revealed that the cycloheptene ring moieties adopt considerably strained twist-boat conformations in which the dihedral angles (θ) of the $-CH_2CH_2-$ bridge are 77.1 and 27.3°, respectively. At 100 °C the α-conformer underwent a one-way conformational inversion to the more stable twist-boat conformer (β-conformer) with an almost *gauche* angle of $\theta = 55.5°$. A kinetic study of the thermal inversion exhibited a small dependency on the quinone substituents as well as negligible solvent effects, providing the transition energy of 127 kJ mol^{-1}. Semiempirical (PM3) calculations were performed to determine the optimized geometries of the α- and β-conformers as well as the inversion transition state structure, which were compared with the X-ray data.

Introduction

Although the conformations of six-membered ring compounds are quite well understood,[1] those of seven-membered rings are substantially more complex due to the extra ring bond which leads to one more degree of torsional freedom as compared with the lower homologue.[2] However, the introduction of strong torsional constraints such as aromatic rings and double bonds results in reduced conformational freedom, as in benzo-,[3] dibenzo-,[4] and tribenzocycloheptenes.[5] Recently, 10,11-dihydro-5*H*-dibenzo[*a*,*d*]cycloheptene **1** and its derivatives have received considerable attention because a variety of pharmacologically active compounds involve such a common subunit suitable for drug–receptor concave–convex interaction.[6]

In a preceding paper, we have reported that 1,3-dipolar cycloaddition of 5-diazo-10,11-dihydro-5*H*-dibenzo[*a*,*d*]cycloheptene **2** with 2-bromo-1,4-naphthoquinone **4c** gave the spirohomonaphthoquinone **7c** in which the spiro-linked 10,11-dihydro-5*H*-dibenzo[*a*,*d*]cycloheptene ring adopts a twist-boat conformation.[7] Interestingly, the first conformer **7c**α (hereafter called the α-conformer; the less stable one) underwent a one-way conformational inversion to the more stable twist-boat form **7c**β (called the β-conformer) at 100 °C (Scheme 1).[7] We have also found that similar reaction of **2** with 2,5-dimethyl-1,4-benzoquinone **3a** provides a sterically congested intermediate (indazole **5a**) which leads to the nitrogen-extruded spirohomobenzoquinone **6a**α at 50 °C (Scheme 2).[8] Here, several questions emerged: (i) why is the less stable α-conformer **7c**α initially formed, (ii) how is the conformation of **5a** related to that of **6a**α, and (iii) whether the α→β conformational inversion also occurs for the homobenzoquinone **6a**α?

In this paper, we will solve the above stereochemical issues on the basis of X-ray crystal structure analyses and PM3 calculations. We also investigated the substituent and solvent effects on the rates of the thermal inversion to gain a deeper insight into the conformational isomerism.

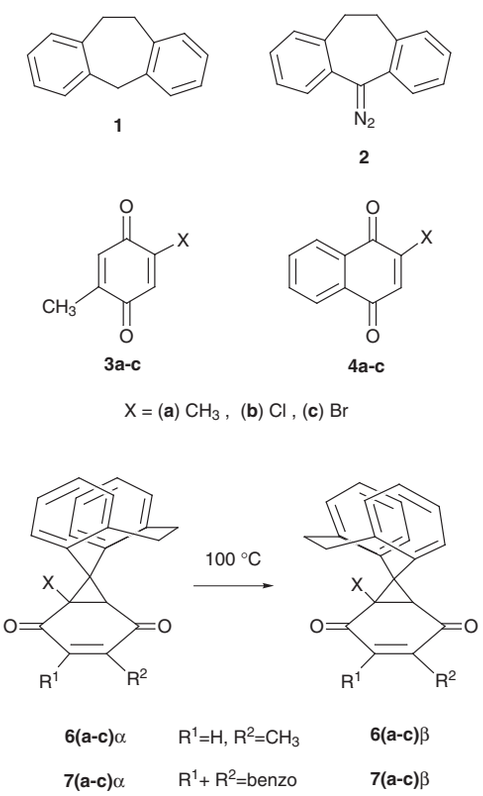

Scheme 1

Results and discussion

Synthesis

The spirohomobenzoquinones **6a**–**c** and spirohomonaphthoquinones **7a**–**c** were prepared by 1,3-dipolar cycloaddition of

† ^{1}H NMR spectra of **6a**α, **6a**β and **7a**α are available as supplementary data from BLDSC (SUPPL. NO. 57566, pp. 4) or the RSC Library. See Instructions for Authors available *via* the RSC web page (http://www.rsc.org/authors).

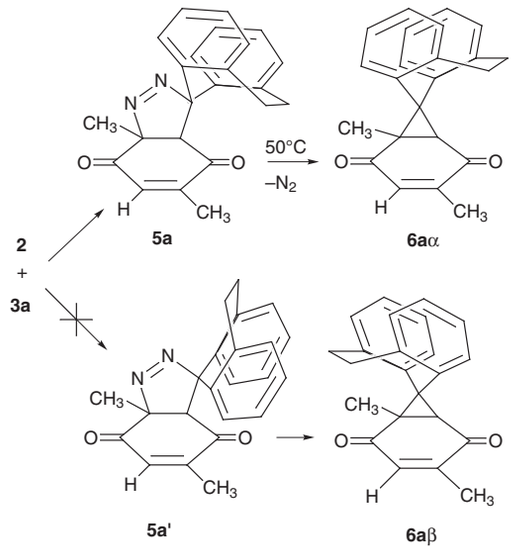

Scheme 2

diazoalkane **2** with the corresponding substituted 1,4-benzoquinones **3a**–**c** and 1,4-naphthoquinones **4a**–**c** *via* spontaneous nitrogen-extrusion of the indazole adducts. As reported previously, only in the reaction with 2,5-dimethyl-1,4-benzoquinone was the indazole **5a** isolated intact along with **6a**α (Scheme 2).[8] The indazole **5a** was regioselectively formed so as to avoid unfavorable steric interactions between the bulky dihydrodibenzo[*a*,*d*]cycloheptene moiety of **2** and the CH_3 substituent at the reacting C=C double bond of quinone.[9] The structures of **5a** and **6a**α were determined by the usual spectroscopic measurements as well as X-ray crystal analyses. No indication of the formation of the respective conformational isomers **5a**′ and **6a**β was obtained upon careful ^{1}H NMR analysis of the crude reaction mixture.

X-Ray crystal structure

Indazole 5a. The X-ray crystal structure of **5a** has been described in our previous paper (triclinic system, space group $P\bar{1}$).[10] Here again, we focus our attention on the conformation of the dihydrodibenzo[*a*,*d*]cycloheptene moiety as compared with that of the nitrogen-extruded spirohomobenzoquinone **6a**α. The seven-membered cycloheptene ring of **5a** has a twist-boat conformation, folding opposite the indazole CH_3 substituent (Scheme 2). The dihedral angle (θ) of the $-CH_2CH_2-$ bridge is 77.1° and the intramolecular bond angle (ω) centered at the spiro-carbon is 117°. Thus, the two benzene rings are fused to the cycloheptene ring with an intersection angle (ψ) of 140°. These conformational properties are listed in Table 1 together with the data for the parent **1** as well as the related compounds. The values of **5a** are much larger than the corresponding values ($\theta = 57.9°$, $\omega = 115°$ and $\psi = 123°$, respectively) of the least strained **1** (selected as the reference compound with an almost *gauche* $-CH_2CH_2-$ bridge).[11] Hence, the two aromatic rings of **5a** are forced out like butterfly wings to avoid steric repulsion from the quinone plane, although several atoms of the seven-membered ring occupy crowded positions almost touching the underlying quinone carbonyl oxygen atom with almost van der Waals distances of 3.2–3.3 Å.[10] Such steric congestion may be responsible for the distorted conformational locking of the dihydrodibenzo[*a*,*d*]cycloheptene ring.[12] It is obvious from the absence of **6a**β that the possible precursor **5a**′ was not formed at all due to the enhanced steric repulsion between the aromatic and quinone moieties.

Spirohomobenzoquinone 6aα. At 50 °C, **5a** slowly loses nitrogen to give rise to spirohomobenzoquinone **6a**α with a half-life period ($t_{1/2}$) of 6.5 h in C_6D_6 (Scheme 2).[8] The structure of **6a**α was determined by X-ray crystallography. Crystals of **6a**α belong to the monoclinic system, with the space group $P2_1/c$. The ORTEP plot showed that the cycloheptene ring still adopts a twist-boat conformation with similar folding opposite the relevant CH_3-substituent (Fig. 1a). However, the relevant angles ($\theta = 27.3°$, $\omega = 108°$ and $\psi = 101°$) are markedly reduced as compared with the precursor **5a** as well as **1**, but are comparable to those of the previously reported **7c**α ($\theta = 28.3°$, $\omega = 109.5°$ and $\psi = 105.5°$) (Table 1).

Table 1 Conformational parameters of the 10,11-dihydro-5*H*-dibenzo[*a*,*d*]cycloheptene rings of crystalline **1**, **5a**, **6a**α, **6a**β and **7c**α

Compound	θ^a (°)	ω^b (°)	ψ^c (°)
1	57.9	114.6	123
5a	77.1	117.3	140
6aα	27.3	107.8	101
6aβ	55.5	111.3	114
7cα	28.3	109.5	106

[a] Dihedral angles of $-CH_2CH_2-$ bridge. $\theta = 1.32\psi - 106$ ($r = 0.964$). [b] C–C–C bond angles centered at the spiro-carbon. $\omega = 0.173\theta + 104$ ($r = 0.966$). [c] Intersection angles of the two aromatic rings. $\psi = 4.01\omega - 333$ ($r = 0.988$).

Mechanistically, it should be noted here that the twist-boat conformation of the seven-membered ring is essentially retained in the nitrogen-extrusion process **5a**→**6a**α, although the dihedral angle of the $-CH_2CH_2-$ bridge is considerably changed. Such a steric outcome in the thermolysis of the indazole is compatible with the general mechanistic considerations arguing for simultaneous homolytic N_2-extrusion followed by a rapid recombination of the nascent diradical.[13,14] In brief, the generation of the less stable α-conformers stems from a reaction sequence involving a sterically restricted 1,3-dipolar addition of diazoalkane **2** with quinones and the conformationally locked nitrogen-extrusion of the indazole adducts.

Spirohomobenzoquinone 6aβ. At 100 °C, **6a**α was transformed to the more stable second conformer (β-conformer). The structure of **6a**β was also determined by X-ray crystallography and the crystal belongs to the orthorhombic system, with the space group *Pccn*. In **6a**β, the cycloheptene ring was inverted close to the cyclopropane CH_3 substituent as seen in the ORTEP drawing (Fig. 1b). The $-CH_2CH_2-$ dihedral angle (θ) of **6a**β is 55.5°, very close to the parent **1** (Table 1),[11] inferring the significant release of strain energy in **6a**α. In addition, the values of ω and ψ are roughly equal to those of **1**. Here, we may compare the solid conformations of the individual dihydrodibenzo[*a*,*d*]-cycloheptene moieties of **1**, **5a**, **6a**α, **6a**β together with **7c**α (Table 1). As seen in the footnotes of Table 1, θ tended to be linearly correlated with ω ($r = 0.966$) and ψ ($r = 0.964$). Another excellent linear relationship was recognized between ω and ψ ($r = 0.988$). These observations are certainly due to the fusion of the two aromatic rings, which considerably constrain the torsional freedom of the cycloheptene ring.

Like **6a**α, the other first conformers **6b**α and **6c**α and **7**(**a**–**c**)α were completely converted to the more stable conformers **6b**β and **6c**β and **7**(**a**–**c**)β at 100 °C *via* the same type of conformational inversion, as confirmed by comparison of the ^{1}H NMR spectral patterns of these pairs of α- and β-conformers (see Experimental section).

Rationale for thermal inversion of 6aα to 6aβ

Comparing the X-ray structures of **6a**α and **6a**β (Fig. 1a,b), we tried to resolve the problem of why the α-conformer is less stable than the β-conformer. Though compound **6a** has two CH_3 groups, the one connected to the cyclopropane ring is expected to play a crucial role in discriminating the conformational stability since the other is more remote from the dihy-

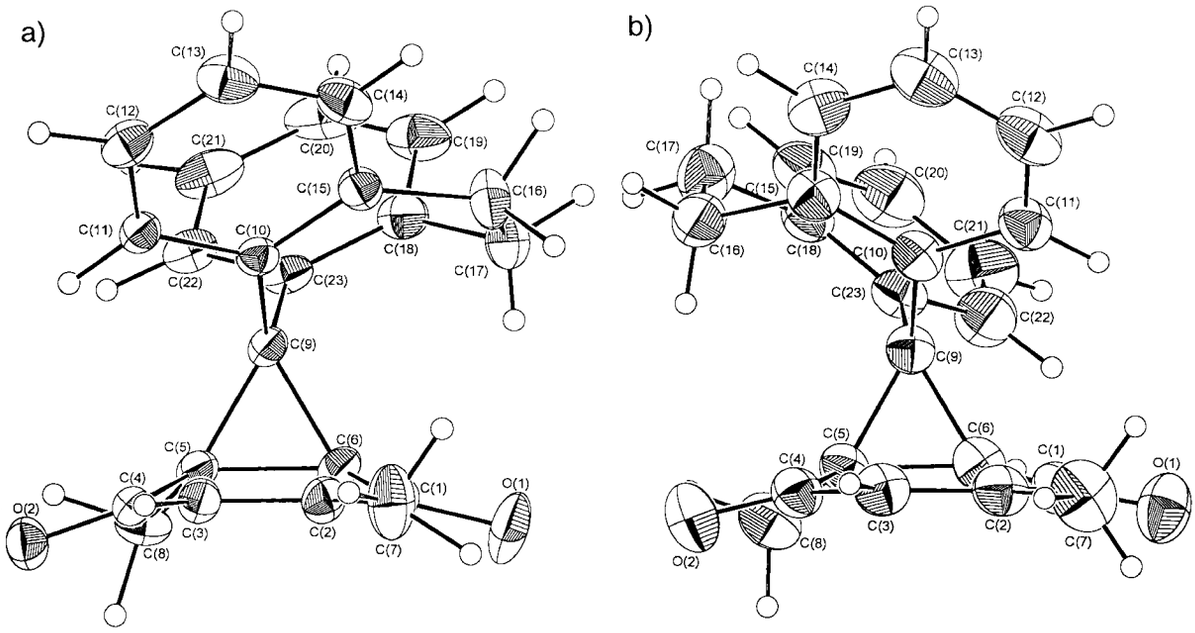

Fig. 1 ORTEP drawing of conformer a) **6a**α and b) **6a**β (ellipsoids at 30% probability).

drodibenzo[*a*,*d*]cycloheptene moiety. This is unambiguously applied for the spirohomonaphthoquinone **7a**, which has only the cyclopropyl CH_3 substituent. A careful perusal of the X-ray structures shows that the CH_3 group of the less stable **6a**α must endure an unfavorable edge-type interaction with the *exo*-aromatic ring (*cis*-aromatic ring to the CH_3 substituent), while that of the stable **6a**β enjoys instead the favorable face-interaction due to the bisected arrangement of the *exo*-aromatic against the cyclopropane ring. This is clearly apparent from a comparison of the dihedral angles of 48.8° (for **6a**α) and 88.4° (for **6a**β), respectively, through the atom sequence C(5) (CH_3-substituted cyclopropane carbon), C(9) (spiro-carbon), C(23) (spiro-linked aromatic), and adjacent aromatic C(22) (for **6a**α) or C(18) (for **6a**β) (Fig. 1a,b). These conformational situations are in harmony with the ^{1}H NMR spectral data (*vide infra*). Our rationalization based on the spatial interaction of the CH_3 with the *exo*-aromatic ring is essentially the same as that invoked by Looker *et al.* for the analogous less stable conformer of 10′,11′-dihydro-2,2-dimethylspiro[cyclopropane-1,5′-(5*H*-dibenzo[*a*,*d*]cycloheptene)] **8**α which was readily inverted to **8**β at 100 °C, moving the methyl groups away from the *peri*-hydrogens of the aromatic rings.[15]

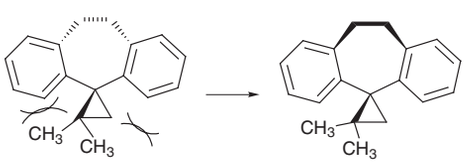

8α **8**β

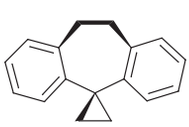

9

NMR Analysis

In conformity with the X-ray analysis, **6a**α and **6a**β showed the characteristic ^{1}H NMR spectra in which the *endo*- and *exo*-aromatic nuclei exerted noticeable diamagnetic anisotropy on the protons of the quinone moieties. Selected chemical shift data are summarized in Table 2. Due to the spatial geometric

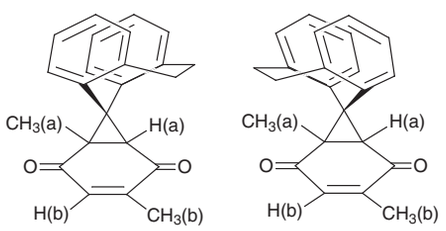

6aα **6a**β

Table 2 Selected ^{1}H NMR chemical shifts of spirohomoquinones **6a**α, **6a**β, **7a**α and **7a**β[a]

	δ/ppm			
Compound	CH_3(a)	H(a)	CH_3(b)	H(b)
6aα	1.69	2.70	1.58[b]	6.26[b]
6aβ	1.25	3.25	1.79[b]	6.02[b]
7aα	1.84	2.89	—	—
7aβ	1.41	3.47	—	—

[a] In $CDCl_3$. [b] Coupling constants are 1.65 Hz.

arrangement of the *exo*-aromatic, **6a**α exhibited a very large downfield shift of 0.44 ppm for the cyclopropyl CH_3(a) and an upfield shift of 0.55 ppm for the cyclopropyl methine proton H(a) with respect to the conformationally inverted **6a**β (δ 1.25 and 3.25 in $CDCl_3$, respectively). The downfield shift reflects the edge interaction and the upfield shift the facial interaction with the *exo*-aromatic ring. Similarly, **7a**α and **7a**β showed almost the same differential chemical shifts of 0.43 and 0.58 ppm for the corresponding cyclopropyl CH_3 and methine proton, although the naphthoquinone aromatic nucleus caused appreciable deshielding shifts (0.15–0.22 ppm) for these protons (Table 2). These spectral data imply that the dihydrodibenzo[*a*,*d*]cycloheptene moieties adopt essentially the same twist-boat conformation in **6a**α and **7a**α, and in **6a**β and **7a**β.

By contrast, although not large, the *endo*-aromatic of **6a**α brought about an upfield shift of 0.21 ppm for CH_3(b) and a downfield shift of 0.24 ppm for vinyl proton H(b) with respect to **6a**β. These opposite and diminished anisotropy effects by the *endo*-aromatic ring are also compatible with the conformations deduced from the X-ray structures.

Table 3 Rate constants (k/s^{-1}) for conformational inversion of **6**(**a**–**c**)α and **7**(**a**–**c**)α in various solvents at 100 °C

Homoquinone	X	Solvent	10^5k/s^{-1}
6aα	CH_3	[$^2H_6$]dimethyl sulfoxide	9.26
		[$^2H_4$]methanol	8.15
		[$^2H_3$]acetonitrile	7.34[a]
		[$^2H_5$]pyridine	6.31
		[$^2H_4$]acetic acid	5.69
		[$^2H_6$]benzene	4.32
		[^{2}H]chloroform	4.05
		carbon tetrachloride	3.31
6bα	Cl	[^{2}H]chloroform	38.4
6cα	Br	[^{2}H]chloroform	41.4
7aα	CH_3	[^{2}H]chloroform	6.62
		[$^2H_3$]acetonitrile	8.01[b]
7bα	Cl	[^{2}H]chloroform	63.2
7cα	Br	[^{2}H]chloroform	66.0

[a] The k values at different temperatures (80 and 90 °C) are 0.887 and 2.61 ($\times10^{-5}$ s^{-1}), respectively, and give the activation parameters ($\Delta H^{\ddagger}$ = 112 kJ mol^{-1}, $\Delta S^{\ddagger}$ = −40.4 J K^{-1} mol^{-1}, $\Delta G^{\ddagger}$ = 127 kJ mol^{-1} at 100 °C). [b] The k values at different temperatures (80 and 90 °C) are 0.993 and 2.85 ($\times10^{-5}$ s^{-1}), respectively, and give the activation parameters ($\Delta H^{\ddagger}$ = 114 kJ mol^{-1}, $\Delta S^{\ddagger}$ = −18.3 J K^{-1} mol^{-1}, $\Delta G^{\ddagger}$ = 121 kJ mol^{-1} at 100 °C).

Kinetic studies

We investigated the effects of substituent and solvent on the rates of the conformational inversion of the α- to the β-conformers. At 80–100 °C in $CDCl_3$, the inversion process was followed by NMR spectrometry until complete conversion to the more stable β-conformers had been achieved. The observed first-order rate constants (k/s^{-1}) for the methyl-, chloro-, and bromo-substituted **6**(**a**–**c**)α and **7**(**a**–**c**)α are given in Table 3. It was found that the homonaphthoquinones **7**(**a**–**c**)α tend to isomerize slightly faster (*ca.* 1.6-fold) than the corresponding homobenzoquinones **6**(**a**–**c**)α. Within each family, the methyl-substituted **6a**α and **7a**α gave inversion rate constants diminished by *ca.* 1/10 compared to the chloro- and bromo-substituted **6b**α, **6c**α and **7b**α, **7c**α, respectively. This rate ratio of 1/10 corresponds to a 7 kJ mol^{-1} higher transition energy for the methyl-substituted spirohomoquinones at 100 °C.

The kinetic substituent effects should be explained by considering the interaction between the *exo*-aromatic ring and the relevant substituents because the *exo*-aromatic is most likely to suffer the substituent steric effects. According to Taft's steric parameters *Es*,[16] CH_3 (−1.24), Br (−1.16), Cl (−0.97), or van der Waals radii,[17] CH_3 (2.23 Å), Br (1.85 Å), Cl (1.75 Å), the most bulky methyl substituent would exert most steric hindrance on the *peri*-hydrogen of the *exo*-aromatic ring in the transition state, raising the activation energy. By contrast, the almost identical rates for the chloro- and bromo-substituted spirohomoquinones may be attributable to a mutual cancellation of steric hindrance between the ground and the transition state or a lack of steric interaction with the *exo*-aromatic ring. Unfortunately, we have no unequivocal explanation for the almost equivalent rates of the Cl- and Br-substituted spirohomoquinones.

Next, the solvent effects were studied for the inversion of the methyl-substituted **6a**α in various deuterated solvents at 100 °C (Table 3). The total variation of k amounts to only a factor of 2.8 over the wide range of solvent polarities investigated. In trend, the rate increases with increasing solvent polarity. But neither the solvent acidity nor the basicity appreciably affected the conversion rate as represented by the rate ratio; $k_{\text{pyridine}}/k_{\text{acetic acid}}$ = 1.1. A plot of log k *vs.* E_{TN} (the normalized polarity parameter based on the transition energy of the Dimroth–Reichardt betaine, widely used as an empirical measure of solvent polarity)[18] provided an insufficient correlation; log $k = 0.479E_{\text{TN}} - 4.42$ (r = 0.75, n = 8). The absence of noticeable kinetic solvent effects is consistent with a mere conformational inversion or with a possible rotation of a biradical intermediate formed by cyclopropane C5–C9 bond scission. It could be argued, however, that a negative $\Delta S^{\ddagger}$ value makes the latter process less likely than a simple conformational flip (*vide infra*).

The activation parameters were obtained for the conformational inversion of the methyl-substituted **6a**α and **7a**α at 100 °C in CD_3CN (footnote in Table 3). The free energies of activation were 127 and 121 kJ mol^{-1}, respectively, and were found to be large enough to isolate each conformer at ordinary temperature. The high $\Delta H^{\ddagger}$ is indicative of a large steric hindrance and the negative $\Delta S^{\ddagger}$ is consistent with highly restricted freedom in the transition state.

Computational studies

Why does the spiro-linkage to the homoquinones cause the conformational locking of the intrinsically interconvertible 10,11-dihydro-5*H*-dibenzo[*a*,*d*]cycloheptene ring? For such a flexible cycloheptene skeleton, an empirical force-field calculation[19] provides interconversion barriers of less than 20 kJ mol^{-1}. However, Looker *et al.* found that spiro-linkage to 1,1-dimethylcyclopropane allowed the separation of two twist-boat conformers **8**α and **8**β at ordinary temperatures, although they did not obtain the inversion barrier.[15] We carried out the PM3 calculation[20] for the spiro-linked model compound **9** in order to estimate the inversion barrier. The calculation yielded a minimum energy twist-boat conformer (θ = 56°) and a transition energy of 41.5 kJ mol^{-1} for the mutual inversion through the highly twisted chair conformation (87°) (Table 4). This barrier appears to be insufficiently high for conformational fixing at ordinary temperature. Therefore, the acquisition of the transition barriers greater then 100 kJ mol^{-1} for **6a**α and **7a**α should be ascribed to the spiro-linkage to the homoquinones. Whereby the steric repulsion would be produced in the transition states between the *endo*-aromatic ring and the quinone plane as well as between the *exo*-aromatic ring and the cyclopropyl substituent. In addition, it is inferred that the α-conformers are considerably less stable than the β-conformers in view of the one-way conformational inversion.

To assess these steric and thermodynamic features, the minimum energy geometries of **6a**α and **6a**β and the inversion transition structure were also provided by semiempirical (PM3) calculation (Fig. 2, Table 4). Species **6a**α is calculated to be higher in energy by 10.9 kJ mol^{-1} than **6a**β, which corresponds to a thermal equilibration of >99:1 in harmony with the experimental one-way inversion. The energy gap is reflected in the dihedral angles, *i.e.* **6a**α (42°) is more strained than **6a**β with a *gauche* angle (57°). In comparison with the X-ray data, the calculated θ noticeably increased by 15° for **6a**α, while it slightly increased by 2° for **6a**β.

The **6a**α to **6a**β transition state was evaluated to be higher in energy by 98 kJ mol^{-1} than the ground state **6a**α. The steric energy increment is roughly comparable to the kinetic result, $\Delta H^{\ddagger}$ (112 kJ mol^{-1}). As noted by the very short interatomic distance of 2 Å between the *peri*-hydrogen H(11) of the *endo*-aromatic ring and the quinone carbonyl carbon C(4) (numbering of atoms is identical to that of the X-ray structure), the transition state endures considerable steric repulsion between the *endo*-aromatic ring and the quinone plane. This steric hindrance will contribute to the high transition energies for the conformational inversion of 10,11-dihydro-5*H*-dibenzo[*a*,*d*]-cycloheptene rings spiro-linked to homoquinones.

Conclusions

We have found that 1,3-dipolar cycloaddition of **2** with variously substituted 1,4-benzoquinones and 1,4-naphthoquinones gave the less stable conformers (called α-conformer) of **6** and **7**

Table 4 Heat of formation, dihedral angles, and interatomic distances of optimized **6a**α, **6a**β, **9** and inversion transition structures

Compound	Heat of formation/ kJ mol^{-1}	Dihedral angle[a] θ/(°)	Interatomic distances/Å H(11)–C(1)[b]	H(11)–C(4)[b]
6aα	67.5	41.7 (27.3)[c]	4.25 (4.31)[c]	2.51 (2.53)[c]
6aβ	56.6	57.4 (55.5)[c]	2.55 (2.59)[c]	4.25 (4.23)[c]
TS‡[d] (**6a**α→**6a**β)	165.3	92.7	3.33	1.97
9	279.0	55.6	—	—
TS‡[d] (**9**⇄**9**)	320.5	87.2	—	—

[a] Dihedral angles of the $-CH_2CH_2-$ bridge. [b] The numbering of atoms is identical to that of the X-ray structures (see Fig. 1). [c] The values in parentheses are the corresponding values of the X-ray analyses (see Fig. 1). [d] TS‡ = Transition state for conformational inversion.

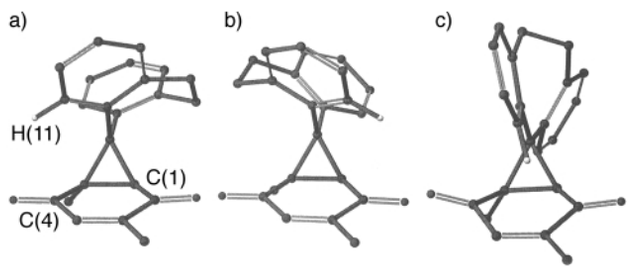

Fig. 2 Ground state structures of a) **6a**α, b) **6a**β and c) inversion transition state structure (numbering of atoms as in Fig. 1).

via a conformationally locked nitrogen-extrusion from the sterically congested indazoles. On heating (100 °C) these α-conformers were completely transformed into the more stable twist-boat conformers (β-conformers) *via* an inversion of the dihydrodibenzo[*a*,*d*]cycloheptene ring. X-Ray analyses revealed that the α-conformer adopts a considerably strained twist-boat ring conformation as compared with the β-conformer as indicated by the dihedral angles (θ) of the $-CH_2CH_2-$ bridge; 27.3° and 55.5°, respectively. The strain in the α-conformer was due to the unfavorable steric interaction between the *exo*-aromatic and the quinone substituents. Kinetic studies indicated that the conformational inversion suffers no appreciable substituent and solvent effects, although the transition energies are greater than 120 kJ mol^{-1}. Empirical PM3 calculations were performed, supporting these experimental results.

Experimental section

Melting points were taken on a Yanagimoto micro-melting point apparatus and are uncorrected. ^{1}H and ^{13}C NMR spectra were obtained on a JEOL EX-270MHz instrument with $Si(CH_3)_4$ (δ 0.00) as internal standard; *J* values are given in Hz. IR spectra were recorded on Perkin-Elmer 983G and JASCO FT/IR-300E spectrometers. Mass spectra were taken on a JEOL JMS DX303 mass spectrometer. Reaction temperatures for the kinetic measurements were controlled by a EYELA NTB-221 thermo-bath.

X-Ray crystallography

Crystal data for 6aα. $C_{23}H_{20}O_2$, $M = 328.41$, monoclinic, space group $P2_1/c$, $a = 14.601(5)$, $b = 9.958(2)$, $c = 12.509(7)$ Å, $\beta = 109.35(3)°$, $V = 1716(1)$ Å^3, $Z = 4$, μ(Mo-Kα) = 0.080 mm^{-1}. A total of 2904 reflections ($R_{int} = 0.113$) were measured on a Mac Science MXC3 diffractometer using graphite-monochromated Mo-Kα radiation at room temperature; 2273 with $I > 2\sigma(I)$ were used in the refinement on *F*. The structure was solved by SHELX-86 and refined by full-matrix least-squares. The refinement converged at $R = 0.069$, $R_w = 0.077$.‡

Crystal data for 6aβ. $C_{23}H_{20}O_2$, $M = 328.41$, orthorhombic, space group *Pccn*, $a = 15.689(5)$, $b = 25.081(8)$, $c = 8.880(3)$ Å, $V = 3494(2)$ Å^3, $Z = 8$, μ(Mo-Kα) = 0.078 mm^{-1}. A total of 1629 reflections ($R_{int} = 0.019$) were measured on a Mac Science MXC3 diffractometer using graphite-monochromated Mo-Kα radiation at room temperature; 2273 with $I > 2\sigma(I)$ were used in the refinement on F^2. The structure was solved by SHELX-86 and refined by full-matrix least-squares. The refinement converged at $R = 0.095$, $R_w = 0.097$.‡

Kinetic measurements

Thermal conversions of **6**(**a**–**c**)α and **7**(**a**–**c**)α to the corresponding conformational isomers **6**(**a**–**c**)β and **7**(**a**–**c**)β were performed at 80–100 °C in a sealed NMR tube. The varying compositions of the isomers of these reactions were monitored at given time intervals by ^{1}H NMR and were determined on the basis of the integral ratios of the methyl signals for **6a–c** and **7a** and the clearly isolated proton signals of the ethano bridge for **7b**,**c**, respectively. The observed first-order rate constants were obtained by the logarithmic plots of the relative amounts of **6** and **7** against time. A least-squares treatment provided an excellent straight line over the second half lives.

Materials

All deuterium solvents were used as purchased. Benzene used as a preparative solvent was refluxed over lithium aluminium hydride for 1 day and fractionated. The quinones **3a** and **4a** were of commercial origin and were purified by recrystallization from hexane–benzene. The quinones **3b**[21] and **4c**[22] were prepared according to the literature methods. The quinones **3c** and **4b** were provided in a similar manner as described above. 5-Diazo-10,11-dihydro-5*H*-dibenzo[*a*,*d*]cycloheptene **2** was synthesized as described; mp 75 °C (decomp.) [lit., 71 °C (decomp.)].[23]

General procedure for reaction of 2 with quinones

To a stirred solution of **3a** (0.41 g, 3.0 mmol) in benzene (4 cm^3) was added **2** (0.66 g, 3.0 mmol). The solution was left to stand for 10 days in the dark at room temperature. After removal of the solvent under reduced pressure below 30 °C, the slurry reaction mixture was washed with hexane–benzene [1 : 1 (v/v), 5 × 3 cm^3] to leave a solid mixture of indazole **5a** (0.54 g) and **6a**α (0.12 g) (by NMR). This mixture provided pure **5a** (0.45 g, 42%) by fractional crystallization from a mixture of hexane and benzene (1 : 1 by volume). The mother liquor and the washing solution were combined and evaporated *in vacuo* below 30 °C. The pasty residue was column chromatographed on silica gel to give successively 10,11-dihydrodibenzo[*a*,*d*]cyclohepten-5-one (33 mg), unreacted quinone (25 mg), **3a** (0.21 g, 21%), and **6a**α (0.19 g, 18%) with an increasing amount of benzene (50–100%) in hexane as eluent. The spirohomoquinones **6b**α and **6c**α and **7**(**a**–**c**)α were synthesized in a similar manner. The stable conformational isomers **6**(**a**–**c**)β and **7**(**a**–**c**)β were obtained quantitatively by prolonged heating (10 days) of the benzene solutions of the α-conformers at 100 °C in sealed tubes.

‡ CCDC reference number 188/169. See http://www.rsc.org/suppdata/p2/1999/1783 for crystallographic files in .cif format.

The structures of indazole **5a**, and the α- and β-conformers of **6a**–**c**, **7a**–**c** were confirmed by the ^{1}H and ^{13}C NMR, IR, and mass spectra as well as elemental analyses. Coupling patterns in the ^{1}H NMR spectra for the methylene protons in the compounds **5a**, **6a**–**c**, and **7a**–**c** showed complex patterns presumably because of conformational equilibria which are known for the dihydrodibenzocycloheptane ring system[24] (see Supporting Information).

3′a,4′,7′,7′a,10,11-Hexahydro-5′,7′-dimethylspiro[5*H*-dibenzo[*a*,*d*]cycloheptene-5,3′-(3′*H*-indazole)]-4,7-dione 5a. Yield 60%; mp 100 °C (decomp.), pale yellow prisms (hexane–benzene); ν_{max}(KBr)/cm^{-1} 1680, 1485, 1372, 1216, 1132, 995, 893, 788, 765; δ_H($CDCl_3$) 1.30 (3H, d, *J* 1.65), 1.42 (3H, s), 2.83–2.92 (1H, m), 3.05–3.10 (1H, m), 3.29 (1H, s), 3.31–3.35 (1H, m), 4.17–4.27 (1H, m), 6.37 (1H, q, *J* 1.65), 6.67–6.71 (1H, m), 7.02–7.36 (7H, m); δ_C($CDCl_3$) 16.2 (CH_3), 21.1 (CH_3), 31.3 (CH_2), 34.3 (CH_2), 64.0 (CH), 102.4 (C_q), 108.0 (C_q), 125.5, 126.0, 126.4, 127.3, 128.5, 128.7, 130.3, 132.58, 132.6, 135.0, 139.5, 140.0, 141.1, 154.6, 189.7 (C=O), 195.4 (C=O) (Found: C, 77.75; H, 5.92; N, 7.69. Calc. for $C_{23}H_{20}O_2N_2$: C, 77.51; H, 5.66; N, 7.86%).

10′,11′-Dihydro-1,4-dimethylspiro[bicyclo[4.2.0]hept-3-ene-7,5′-(5′*H*-dibenzo[*a*,*d*]cycloheptene)]-2,5-dione 6aα. Yield 21%; mp 192–193 °C, pale yellow prisms (hexane–benzene); ν_{max}(KBr)/cm^{-1} 1670, 1594, 1336, 1298, 763, 753; δ_H($CDCl_3$) 1.58 (3H, d, *J* 1.65), 1.69 (3H, s), 2.70 (1H, s), 2.80–2.96 (2H, m), 3.23–3.32 (1H, m), 4.00–4.13 (1H, m), 6.26 (1H, q, *J* 1.65), 6.84–7.02 (4H, m), 7.07–7.24 (4H, m); δ_C15.5 (CH_3), 18.5 (CH_3), 29.9 (CH_2), 30.8 (CH_2), 40.5 (spiro), 47.7 (CH), 50.4 (Cq), 125.6, 126.2, 126.4, 127.6, 127.8, 128.9, 130.4, 131.8, 135.8, 137.2, 138.4, 138.7, 140.9, 147.2, 195.7 (C=O), 197.4 (C=O); *m*/*z* 328 (M^+) (Found: C, 84.06; H, 6.24. Calc. for $C_{23}H_{20}O_2$: C, 84.12; H, 6.14%).

6aβ. Mp 164.5–165 °C, pale yellow prisms (hexane–benzene); ν_{max}(KBr)/cm^{-1} 1672, 1655, 1487, 1458, 1333, 758; δ_H($CDCl_3$) 1.25 (3H, s), 1.79 (3H, d, *J* 1.65), 2.65–2.72 (1H, m), 2.91–2.98 (1H, m), 3.25 (1H, s), 3.44–3.49 (2H, m), 6.02 (1H, q, *J* 1.65), 6.81–6.99 (4H, m), 7.07–7.14 (4H, m).

1-Chloro-10′,11′-dihydro-4-methylspiro[bicyclo[4.2.0]hept-3-ene-7,5′-(5′*H*-dibenzo[*a*,*d*]cycloheptene)]-2,5-dione 6bα. Yield 65%; mp 176–177 °C, pale yellow prisms (hexane–benzene); ν_{max}(KBr)/cm^{-1} 1678, 1592, 1294, 1278, 761; δ_H($CDCl_3$) 1.61 (3H, d, *J* 1.65), 2.82–2.98 (2H, m), 3.20–3.28 (1H, m), 3.25 (1H, s), 3.93–4.06 (1H, m), 6.41 (1H, q, *J* 1.65), 6.85–7.03 (4H, m), 7.61–7.63 (4H, m); *m*/*z* 348 (M^+) (Found: C, 75.68; H, 5.01. Calc. for $C_{22}H_{17}O_2Cl$: C, 75.75; H, 4.91%).

6bβ. Mp 181.0–182.5 °C, pale yellow prisms (hexane–benzene); ν_{max}(KBr)/cm^{-1} 2909, 1677, 1665, 1627, 1485, 1458, 1298, 1128, 899, 779, 761; δ_H($CDCl_3$) 1.84 (3H, d, *J* 1.32), 2.68–2.78 (1H, m), 2.85–3.00 (1H, m), 3.40–3.60 (2H, m), 3.71 (1H, s), 6.19 (1H, q, *J* 1.32), 6.77–7.39 (8H, m).

1-Bromo-10′,11′-dihydro-4-methylspiro[bicyclo[4.2.0]hept-3-ene-7,5′-(5′*H*-dibenzo[*a*,*d*]cycloheptene)]-2,5-dione 6cα. Yield 55%; mp 175–177 °C, pale yellow prisms (hexane–benzene); ν_{max}(KBr)/cm^{-1} 1676, 1591, 1293, 1277, 760; δ_H($CDCl_3$) 1.62 (3H, d, *J* 1.65), 2.82–2.97 (2H, m), 3.19–3.28 (1H, m), 3.26 (1H, s), 3.94–4.07 (1H, m), 6.42 (1H, q, *J* 1.65), 6.86–7.04 (4H, m), 7.62–7.64 (4H, m); *m*/*z* 392 (M^+) (Found: C, 67.40; H, 4.52. Calc. for $C_{22}H_{17}O_2Br$: C, 67.19; H, 4.36%).

6cβ. Mp 177–178 °C, pale yellow prisms (hexane–benzene); ν_{max}(KBr)/cm^{-1} 2909, 1673, 1663, 1626, 1484, 1459, 1356, 1283, 1227, 1126, 899, 780, 760; δ_H($CDCl_3$) 1.84 (3H, d, *J* 1.65), 2.67–2.75 (1H, m), 2.90–2.97 (1H, m), 3.42–3.60 (2H, m), 3.75 (1H, s), 6.20 (1H, q, *J* 1.65), 6.70–7.01 (4H, m), 7.08–7.36 (4H, m).

10′,11′-Dihydro-1a-methylspiro[1*H*-cyclopropa[*b*]naphthalene-1,5′-(5′*H*-dibenzo[*a*,*d*]cycloheptene)]-2,7-dione 7aα. Yield 72%; mp 181–182 °C, colorless prisms (hexane–benzene); ν_{max}(KBr)/cm^{-1} 1670, 1594, 1336, 1298, 763, 753; δ_H($CDCl_3$) 1.84 (3H, s), 2.89 (1H, s), 2.75–2.97 (2H, m), 3.27–3.68 (1H, m), 4.12–4.25 (1H, m), 6.50–6.56 (2H, m), 6.64–6.72 (2H, m), 6.91–6.94 (3H, m), 7.26–7.52 (3H, m), 7.93–7.96 (1H, m), 8.10–8.13 (1H, m); *m*/*z* 364 (M^+) (Found: C, 85.92; H, 5.77. Calc. for $C_{26}H_{20}O_2$: C, 85.69; H, 5.53%).

7aβ. Mp 182–183 °C, colorless prisms (hexane–benzene); ν_{max}(KBr)/cm^{-1} 1673, 1662, 1592, 1487, 1459, 1325, 1300, 1244, 970, 756, 743; δ_H($CDCl_3$) 1.41 (3H, s), 2.63–2.71 (1H, m), 2.83–2.96 (1H, m), 3.47 (1H, s), 3.42–3.68 (2H, m), 6.53–6.58 (1H, m), 6.75–6.81 (2H, m), 6.89–6.92 (1H, m), 7.03–7.19 (3H, m), 7.35–7.52 (3H, m), 7.63–7.66 (1H, m), 7.91–7.95 (1H, m).

1a-Chloro-10′,11′-dihydrospiro[1*H*-cyclopropa[*b*]naphthalene-1,5′-(5′*H*-dibenzo[*a*,*d*]cycloheptene)]-2,7-dione 7bα. Yield 67%; mp 173–174 °C, colorless prisms (hexane–benzene); ν_{max}(KBr)/cm^{-1} 1678, 1592, 1294, 1278, 761; δ_H($CDCl_3$) 2.77–3.00 (2H, m), 3.24–3.34 (1H, m), 3.40 (1H, s), 4.08–4.21 (1H, m), 6.54–8.06 (12H, m); *m*/*z* 384 (M^+) (Found: C, 78.03; H, 4.57. Calc. for $C_{25}H_{17}O_2Cl$: C, 78.02; H, 4.45%).

7bβ. Mp 203–204 °C, colorless prisms (hexane–benzene); ν_{max}(KBr)/cm^{-1} 2893, 1592, 1487, 1350, 1290, 1214, 768, 753, 729; δ_H($CDCl_3$) 2.69–2.77 (1H, m), 2.84–2.99 (1H, m), 3.57–3.69 (2H, m), 3.93 (1H, s), 6.55–6.60 (1H, td, J_1 7.59, J_2 1.32), 6.72–6.75 (1H, dd, J_1 7.59, J_2 1.32), 6.80–6.86 (1H, td, J_1 7.59, J_2 1.32), 6.93–6.96 (1H, d, *J* 7.59), 7.09–7.13 (1H, m), 7.15–7.36 (2H, m), 7.42–7.50 (2H, m), 7.54–7.60 (1H, m), 7.72–7.75 (1H, dd, J_1 7.59, J_2 1.32), 7.97–8.00 (1H, dd, J_1 6.92, J_2 1.32).

1a-Bromo-10′,11′-dihydrospiro[1*H*-cyclopropa[*b*]naphthalene-1,5′-(5′*H*-dibenzo[*a*,*d*]cycloheptene)]-2,7-dione 7cα. Yield 63%; mp 173–175 °C, colorless prisms (hexane–benzene); ν_{max}(KBr)/cm^{-1} 1676, 1591, 1293, 1277, 760; δ_H($CDCl_3$) 2.77–2.99 (2H, m), 3.23–3.33 (1H, m), 3.47 (1H, s), 4.07–4.20 (1H, m), 6.54–6.75 (3H, m), 6.95 (1H, d, *J* 7.60), 7.17–7.20 (3H, m), 7.44–7.57 (2H, m), 7.67–7.71 (1H, m), 7.78 (1H, q, J_1 5.60, J_2 1.32), 8.03 (1H, q; J_1 5.60, J_2 1.32); *m*/*z* 428 (M^+) (Found: C, 69.93; H, 4.12. Calc. for $C_{25}H_{17}O_2Br$: C, 69.94; H, 3.99%).

7cβ. Mp 191–193 °C, colorless prisms (hexane–benzene); ν_{max}(KBr)/cm^{-1} 1677, 1591, 1283, 757; δ_H($CDCl_3$) 2.67–2.76 (1H, m), 2.85–2.98 (1H, m), 3.58–3.74 (2H, m), 3.97 (1H, s), 6.53–6.59 (1H, t, *J* 7.59), 6.72–6.74 (1H, d, *J* 7.61), 6.79–6.88 (1H, d, *J* 7.61), 6.94–6.97 (1H, d, *J* 7.59), 7.09–7.24 (3H, m), 7.41–7.59 (3H, m), 7.71–7.74 (1H, m), 7.97–8.00 (1H, m).

References

1 (*a*) O. Hassel, *Quart. Rev.*, 1953, **7**, 221; (*b*) E. L. Eliel, *Stereochemistry of Carbon Compounds*, McGraw Hill, New York, 1962; (*c*) F. G. Riddlell, *The Conformational Analysis of Heterocyclic Compounds*, Academic Press, New York, 1980; (*d*) E. J. Corey and N. F. Feiner, *J. Org. Chem.*, 1980, **45**, 765; (*e*) R. Aydin and H. Gunter, *Angew. Chem., Int. Ed. Engl.*, 1981, **20**, 985; (*f*) N. L. Allinger, Y. H. Yuh and J.-H. Lii, *J. Am. Chem. Soc.*, 1989, **111**, 8551; (*g*) J.-H. Lii and N. L. Allinger, *J. Am. Chem. Soc.*, 1989, **111**, 8566; (*h*) D. M. Ferguson and D. J. Raber, *J. Am. Chem. Soc.*, 1989, **111**, 4371; (*i*) H. Goto and E. Osawa, *J. Am. Chem. Soc.*, 1989, **111**, 8950; (*j*) D. A. Dixon and A. Komornicki, *J. Am. Chem. Soc.*, 1990, **94**, 5630; (*k*) A. Bejer and P. Schuster, *Monatsh. Chem.*, 1990, **121**, 339; (*l*) *Second Supplement to the 2nd Edition of Rodd's Chemistry of Carbon Compounds*, ed. M. Sainsbury, Elsevier, Amsterdam, 1992, vol. IIA/B, ch. 1.

2 (*a*) J. B. Hendrickson, *J. Am. Chem. Soc.*, 1967, **89**, 7043; (*b*) J. Dillen and H. J. Geise, *J. Chem. Phys.*, 1979, **70**, 424; (*c*) M. A. Winnik, *Chem. Rev.*, 1981, **81**, 491; (*d*) P. J. DeClerq, *J. Org. Chem.*, 1981, **46**, 667; (*e*) A. L. Esteban, C. Galiano, E. Diez and F. J. Bermejo, *J. Chem. Soc., Perkin Trans. 2*, 1982, 657; (*f*) G. Favini, *J. Mol.*

Struct., 1983, **93**, 139; (*g*) V. Elser and H. L. Strauss, *Chem. Phys. Lett.*, 1983, **96**, 276; (*h*) O. V. Dorofeeva, L. V. Gurvich and V. S. Mastryukov, *J. Mol. Struct.*, 1985, **129**, 165; (*i*) F. A. L. Anet, *Conformational Analysis of Medium-Sized Heterocycles*, ed. R. S. Glass, VCH, New York, 1988, ch. 2; (*j*) D. Cremer, *J. Phys. Chem.*, 1990, **94**, 5502.
3 E. Grunwald and E. Price, *J. Am. Chem. Soc.*, 1965, **87**, 3139.
4 W. Weissensteiner, O. Hofer and U. G. Wagner, *J. Org. Chem.*, 1988, **53**, 3988.
5 M. Nógrádi, W. D. Ollis and I. O. Sutherland, *J. Chem. Soc.*, *Chem. Commun.*, 1970, 158.
6 A. Burger, *A Guide to the Chemical Basis of Drug Design*, Wiley, New York, 1983.
7 H. Tamura, T. Oshima, G. Matsubayashi and T. Nagai, *Acta Crystallogr.*, *Sect. C*, 1995, **51**, 1148.
8 T. Oshima and T. Nagai, *J. Chem. Soc.*, *Chem. Commun.*, 1994, 2787.
9 R. Huisgen, *1,3-Dipolar Cycloaddition Chemistry*, ed. A. Padwa, John Wiley & Sons, New York, 1984, vol. I, pp. 1–176.
10 T. Oshima, T. Kawamoto, H. Kuma, Y. Kushi and T. Nagai, *J. Chem. Soc.*, *Chem. Commun.*, 1995, 1937.
11 P. J. P. Reboul and B. Cristau, *Acta Crystallogr.*, *Sect. B*, 1981, **37**, 394.
12 In ^{1}H NMR measurements, diazoalkane **1** showed one sharp singlet at δ 2.72 ($CDCl_3$) for the $–CH_2CH_2–$ bridging, indicating rapid interconversion of the dihydrodibenzocycloheptene moiety in NMR time scale.
13 (*a*) D. S. Wulfman, G. Linstrumelle and C. F. Cooper, *Synthetic Application of Diazoalkanes*, in *The Chemistry of Diazonium and Diazo Groups*, *Part 2*, ed. S. Patai, Wiley, New York, 1978, p. 821; (*b*) Y. Nakano, M. Hamaguchi and T. Nagai, *J. Org. Chem.*, 1989, **54**, 1135 and references cited therein.
14 (*a*) H. Meier and K.-P. Zeller, *Angew. Chem.*, *Int. Ed. Engl.*, 1977, **16**, 835; (*b*) P. S. Engel, *Chem. Rev.*, 1980, **80**, 99.
15 J. J. Looker, D. P. Maier and T. H. Regan, *J. Org. Chem.*, 1972, **37**, 3401.
16 S. H. Unger and C. Hanasch, *Prog. Phys. Org. Chem.*, 1976, **12**, 91.
17 M. Charton, *J. Am. Chem. Soc.*, 1969, **91**, 615.
18 (*a*) C. Reichardt and E. H.-Görnert, *Liebigs Ann. Chem.*, 1983, 721; (*b*) C. Reichardt, *Chem. Rev.*, 1994, **94**, 2319.
19 According to the empirical force-field calculation, Weissensteiner *et al.* reported that 10,11-dihydro-5*H*-dibenzo[*a*,*d*]cycloheptene **1** interconverts *via* a C_2- or C_s-symmetrical transition state with an energy of 19.7 or 16.9 kJ mol^{-1} relative to the ground state of C_1 symmetry, see ref. 4.
20 The calculations using the PM3 method were performed with the MOPAC program (ver. 6) using a Cache Work-System.
21 J. Cason, C. F. Allen and S. Goodwin, *J. Org. Chem.*, 1948, **13**, 403.
22 T. Zincke and M. Schmidt, *Ber.*, 1895, **28**, 2753.
23 I. Moritani, S. Murahashi, K. Yoshinaga and H. Ashitaka, *Bull. Chem. Soc. Jpn.*, 1967, **40**, 1506.
24 R. J. Abraham, L. J. Kricka and A. Ledwith, *J. Chem. Soc.*, *Perkin Trans. 2*, 1974, 1648.

Paper 9/00475K